V European Conference on Computational Fluid Dynamics
ECCOMAS CFD 2010
J. C. F. Pereira and A. Sequeira (Eds)
Lisbon, Portugal,14-17 June 2010

STUDYING SWIRLING FLAMES USING HIGHLY RESOLVED SIMULATIONS OF AN INDUSTRIAL PREMIXED BURNER

V. Moureau*, P. Domingo* and L. Vervisch*

*CORIA - CNRS and INSA de Rouen,
76801 Saint-Etienne-du-Rouvray, France
e-mail: vincent.moureau@coria.fr

Key words: premixed turbulent combustion, large-eddy simulation, direct numerical simulation, PCM-FPI

Abstract. *In this paper, Large-Eddy Simulations (LES) and Direct Numerical Simulation (DNS) are applied in the analysis of an industrial swirl burner operated with a lean methane-air mixture. LES is used to study the mesh convergence of the species and temperature statistics, while DNS allows to gain insight into the flame structure and dynamics. The DNS features a 2.6 billion cell unstructured-mesh and a resolution of 100 microns and is sufficient to capture all the turbulent scales and the major species of the flame brush, while the unresolved species are taken into account thanks to a tabulated chemistry approach. Finally, the DNS is filtered at several filter widths to validate the PCM-FPI combustion model. All these simulations are performed with a novel solver specifically tailored for large scale computations on massively parallel machines.*

1 Introduction

1.1 Motivation

In turbulent premixed flames, reactions occur in very thin regions that are typically one to two orders of magnitude smaller than the mesh resolutions used in industry for combustion-chamber design. This makes the modeling of premixed flames a challenging issue. To gain insight into the dynamics of premixed flames, it would be convenient to have access to simulations of realistic devices at moderate Reynolds numbers, where all the dynamics of turbulence and of major species would be resolved. Intermediate radical species could be obtained from chemistry tabulation, since their very accurate prediction may not always be of primary importance on the global dynamics of the flame. The tabulated-chemistry models based on the flamelet assumption are particularly well suited for this type of computations, since the evolution of all the species and source terms are mapped onto control parameters, such as mixture fraction and progress variable for partially premixed flames, that may be computed from major species. For industrial devices, the main point that needs to be addressed, is the prohibitive cost of such computations, which may be referred to as direct numerical simulations (DNS), since all the turbulent eddies and their interactions with the flame are resolved. In this paper, a mesh refinement study based on LES and DNS of an industrial premixed burner is presented for steady operating conditions. These computations are performed with a finite-volume LES/DNS solver specifically tailored for large-scale computations of turbulent reacting flows in realistic geometries.

1.2 Methodology

The main issue of DNS comes from the wide range of scales that need to be resolved. On the one hand, the flow rate and the large scales of the flow must be statistically converged and, on the other hand, the smallest scales, namely the Kolmogorov scale and the flame brush thickness, must be also resolved. Obviously, the convergence of the flow rate and the large eddies may be obtained with large-eddy simulations (LES) on relatively coarse meshes, while the access to the smallest scales requires DNS. From this principle, the presented methodology consists of successive LES of increasing resolution up to DNS. A first coarse mesh, fine enough to correctly describe the full geometry, is used to perform a very large-eddy simulation (VLES). This enables to settle the flow rate, the large scales and the mean flame brush. Then, this coarse solution is interpolated on a finer mesh. The convergence of the turbulent scales on this finer mesh may be achieved after approximately several eddy turn-over time of the smallest scales resolved on the coarse mesh. This eddy turn-over time is considerably smaller than the time required to settle the flow rate and the energetic scales, because the size of these eddies is a fraction of the one of the large scales. This operation is repeated until all scales of interest are resolved, thus reaching DNS resolution. In the paper, a mesh refinement study is performed with LES computations of increasing resolution. This study allows to show the statistical convergence of the mean and rms quantities. Then, the mesh is further refined to perform the DNS of the reacting flow without any turbulence model. The initial condition of the DNS is given by the finest LES computations in order to save a great amount of CPU time, and the DNS run is

pursued long enough to evacuate possible errors remaining from LES. From this DNS, the flame structure is studied and some instantaneous fields are filtered to bring valuable informations for LES modeling.

1.3 Geometry and operating conditions

The experimental configuration chosen in this paper is the so-called PRECCINSTA burner (Lartigue *et al.*, 2004; Meier *et al.*, 2007), which was designed by Turboméca, SAFRAN group, in the PRECCINSTA european project. Its focus is the validation of large-eddy simulation models in realistic conditions. This geometry has been widely used as a validation database for combustion models (Galpin *et al.*, 2008; Roux *et al.*, 2005; Moureau *et al.*, 2007*b*) or for numerical methods applied to the solving of the Navier-Stokes equations (Moureau *et al.*, 2007*a*).

The geometry considered in the simulations, presented in Fig. 1, features a plenum, a swirler, a square combustion chamber and a cylindrical exhaust pipe. The burner is fed steadily with a mixture of methane and air at an equivalence ratio of 0.83, and the total mass flow rate is $12.9\,\mathrm{g/s}$.

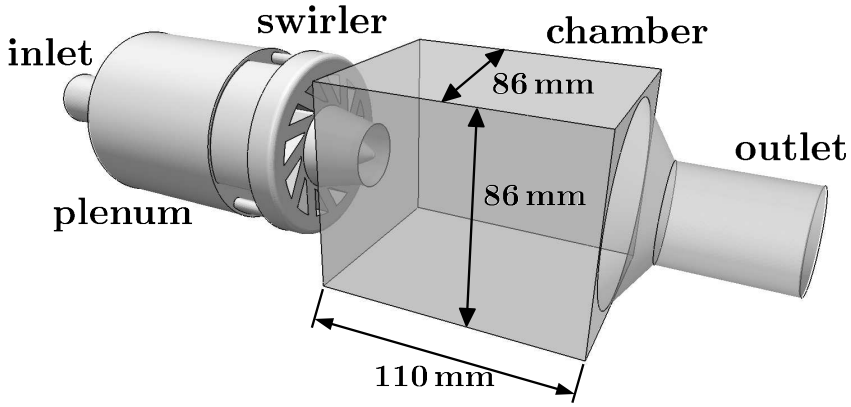

Figure 1: Computed geometry of the PRECCINSTA burner.

1.4 Turbulence and flame parameters

The mesh requirements for the DNS are mainly determined by the turbulence and flame parameters in the fresh gases at the swirler exit. In the burned gases, the increased kinematic viscosity leads to an important decrease of the turbulent Reynolds number and an increase of the Kolmogorov length scale, so that they do not have to be considered for the mesh requirements. Concerning the turbulence parameters, the Reynolds number based on the mean velocity and the pipe diameter is approximately $Re = 40000$. The turbulent velocity u' at the swirler exit may be estimated from the azimuthal velocity which doesn't feature any steep gradient that would generate intermittency and increase the rms. These azimuthal fluctuations may thus be considered to be a good estimate of u'. From the different LES computations and from the

	1.7M	14M	110M	329M
$\Delta\,[\mathrm{mm}]$	1.2	0.6	0.3	0.2
δ_T/Δ	5.8	11.7	23.3	35.0
Δ/η	41.4	20.7	10.3	6.9
δ_L/Δ	0.35	0.71	1.41	2.12

Table 1: Resolution parameters for the LES computations

experimental measurements, $u' = 3.5\,\mathrm{m/s}$. Then, the turbulent dissipation may be measured from the turbulent viscosity in the LES computations presented thereafter: $\epsilon = 6100\,\mathrm{m^2/s^3}$. The turbulent dissipation and the velocity fluctuations give an estimate of the integral length scale $\delta_T = u'^3/\epsilon = 7.0\,\mathrm{mm}$ and of the integral eddy-turnover time $\tau_T = \delta_T/u' = 2\,\mathrm{ms}$. The dissipation also allows to estimate the Kolmogorov length scale $\eta = (\nu^3/\epsilon)^{(1/4)} = 29\mu\mathrm{m}$, the turbulent Reynolds number $Re_t = 1480$, and the Reynolds number based on the Taylor length scale $Re_\lambda = 149$. Another important scale of the PRECCINSTA burner is the Precessing Vortex Core that has a frequency around $540\,\mathrm{Hz}$. This leads to a characteristic time scale of $1.9\,\mathrm{ms}$ close to the integral time scale.

Concerning the premixed flame parameters, the laminar flame speed in the unburned gases is $s_L = 0.293\,\mathrm{m/s}$, while its diffusive thickness is $\delta = 0.078\,\mathrm{mm}$. This diffusive thickness is not relevant for the mesh requirements (Poinsot & Veynante, 2001), unlike the thermal thickness $\delta_L = 0.424\,\mathrm{mm}$, which is based on the maximum temperature gradient. The turbulence and flame parameters leads to Damköhler and Karlovitz numbers: $Da = (\delta_T/u')/(\delta/s_L) = 7.51$ and $Ka = (\delta/\eta)^2 = 7.23$. The Karlovitz number indicates that the combustion regime is the thin reaction zones regime in agreement with (Moureau *et al.*, 2007*b*).

2 Mesh refinement study with Large-Eddy Simulations

2.1 Description

For this realistic burner, LES is performed successively on meshes with 1.7, 14, 110, and 329 million tetrahedrons. The resolution of the meshes and the ratios with the turbulence and flame length scales are presented in Table 1. The results of the 329 million tetrahedrons are not presented in this section because the mean and rms profiles are not converged enough. This computation is mentioned because it is used to initialize the DNS computation presented thereafter.

To save a great amount of CPU time, all the LES, except the coarsest one, are initialized with the fields of the previous LES in terms of resolution. This interpolation may be of low order since the fields are then statistically converged at each refinement step, but it has to be performed in parallel with meshes of increasing size. Another important point of this mesh refinement study is the mesh generation. To reach fine LES and DNS of turbulent combustion in realistic burners, the mesh resolution has to be typically greater than one billion elements. This mesh size can hardly be generated with usual mesh generators that are limited to a hundred

million of elements typically. A solution is the generation of meshes that are fine enough to correctly describe the geometry, and then to apply an homogeneous mesh refinement algorithm that tessellates the elements into smaller elements. Non degenerescent algorithms for tetrahedrons may be used (Rivara, 1984) to insure that the mesh keeps its original quality after successive refinements. Moreover, this processing has to be done in parallel to avoid any memory limitation. The interpolation and mesh refinement algorithms are available in the finite-volume YALES2 solver. This code solves the low-Mach Navier-Stokes equations with a projection method for constant or variable density flows. These equations are discretized with a 4th-order central scheme in space and a 4th-order Runge-Kutta like scheme in time.

2.2 Results

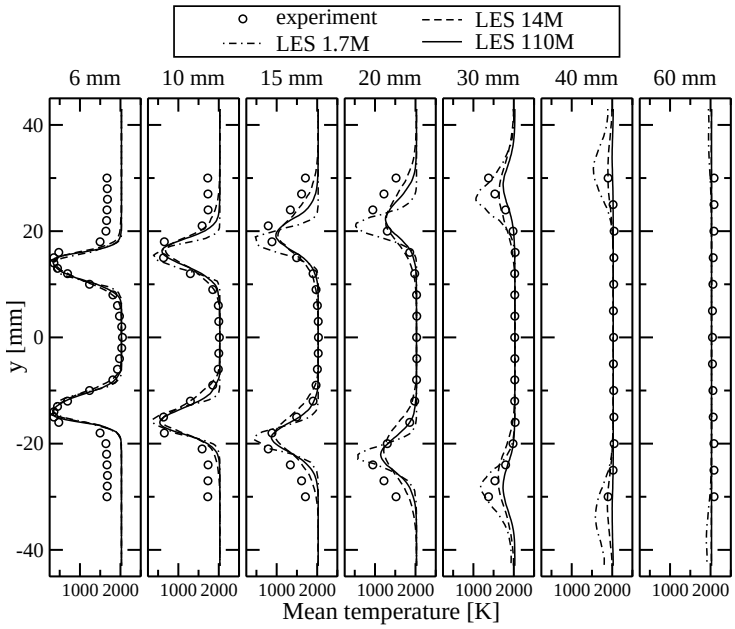

Figure 2: Mesh refinement study with LES. Mean temperature profiles.

The LES computations are performed with the localized dynamic Smagorinsky model Germano *et al.* (1991) and the presumed-pdf combustion model PCM-FPI, based on beta-function and premixed flamelet Domingo *et al.* (2008); Gicquel *et al.* (2000); Van Oijen *et al.* (2001). The unmixedness factor of the progress variable required by the PCM-FPI model is kept constant for each LES, its intensity being lowered as the mesh resolution increases. The chemistry table is built from premixed flames at the given equivalence ratio with the Cantera chemistry software, and the chosen progress variable is $Y_c = Y_{\mathrm{CO}} + Y_{\mathrm{CO_2}}$, while the GRI-3.0 mechanism is used for CH_4-Air combustion Smith *et al.* (1999). For the first three resolutions, the computation time required for accumulating statistics was tractable, which allows for validating the simulations against the Raman measurements performed at DLR in Germany. The averages are

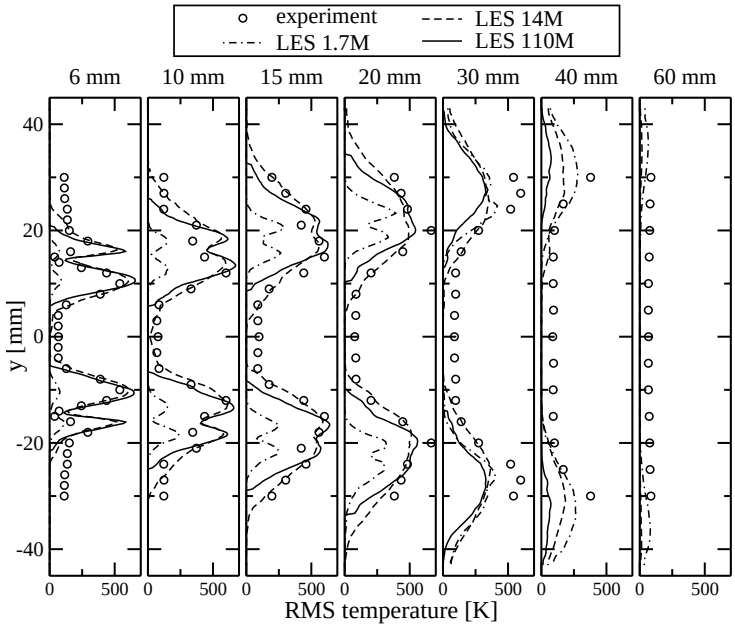

Figure 3: Mesh refinement study with LES. Temperature fluctuations profiles.

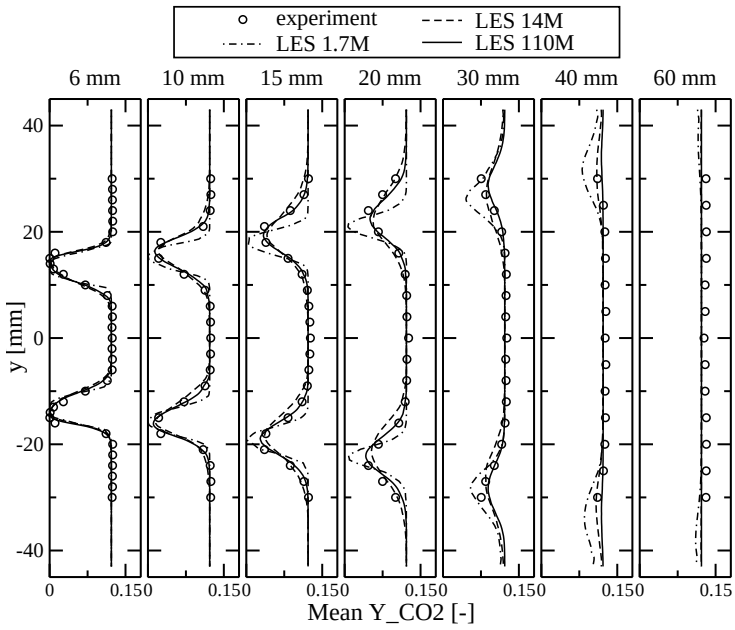

Figure 4: Mesh refinement study with LES. Mean CO_2 profiles.

collected during 240, 90 and 52 ms of physical time for the 1.7, 14 and 110 million cell meshes, respectively. These durations may be compared to the eddy turnover time of $2.0\,\mathrm{ms}$ in the fresh

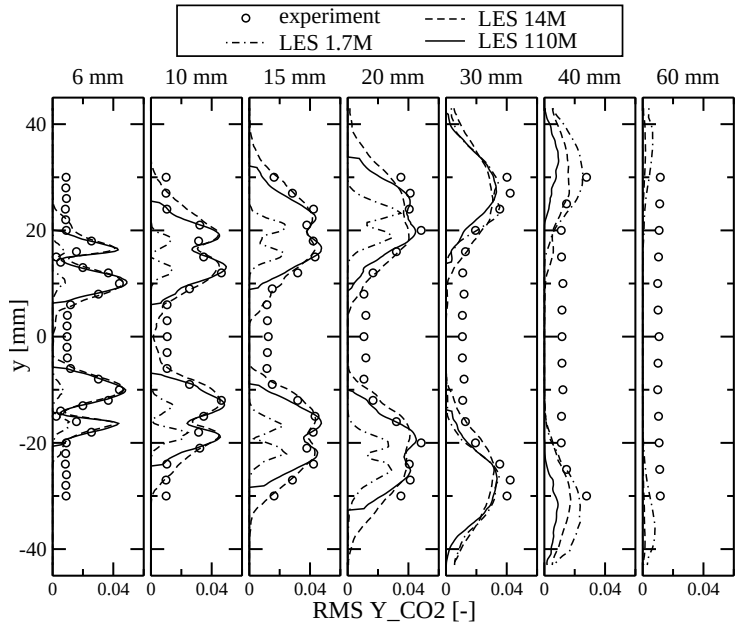

Figure 5: Mesh refinement study with LES. CO_2 fluctuations profiles.

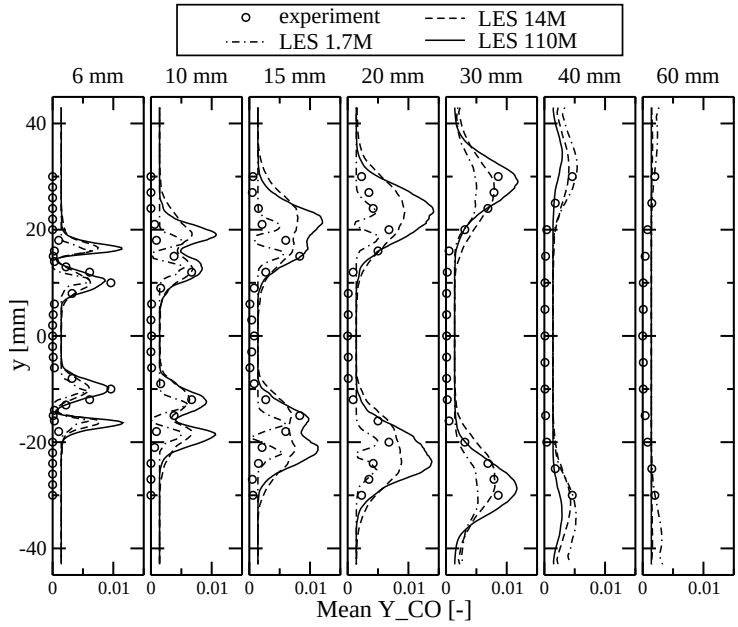

Figure 6: Mesh refinement study with LES. Mean CO profiles.

gases, and to the mean flow-through time in the combustor of the order of 30 ms for the reacting case. Mean and RMS temperature profiles, and CO_2 and CO concentration profiles are given in

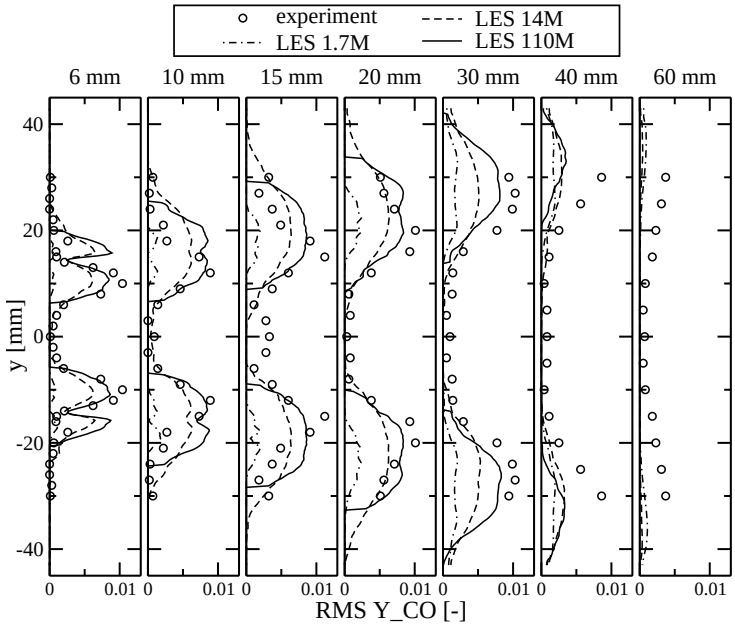

Figure 7: Mesh refinement study with LES. CO fluctuations profiles.

Fig. 2 to 7. These profiles are taken in the median plane at different distances from the swirler exit Galpin *et al.* (2008). First, this comparison highlights the gain obtained with the mesh resolution increase, especially from 1.7 to 14 million cells. Second, the mean and especially the RMS temperature profiles are well predicted on the fine mesh, except in the corner recirculation zones (CRZ) where the temperature is underestimated. As stated by Galpin et al Galpin *et al.* (2008), this difference may be attributed to the dilution of the fresh mixture by burned gases in the CRZ, but in that case it should also be visible in the central recirculation zone. Or, it may be due to heat losses at walls in the corners, since the flow is strongly confined in the CRZ, that would induce a lack of CO recombination as seen in Fig. 7. This phenomenon is not observed on $\mathrm{CO_2}$ since the $\mathrm{CO_2}$ variation that would result of the correct CO recombination, to have the experimental temperature, is negligible compared to $\mathrm{CO_2}$ concentration. Finally, fluctuations of temperature, $\mathrm{CO_2}$ and CO at the 40 mm station are systematically underestimated with the finer mesh. This cannot be explained by a lack of statistical convergence since this convergence was verified by comparing the results after different accumulation times. This configuration is known to have an important 3/4 wave acoustic mode that could explain an increase of all fluctuation levels not captured by the present LES.

3 Direct Numerical Simulation analysis

3.1 Description

The DNS mesh features 2.6 billion tetrahedrons with a resolution Δ_{DNS} of 100 $\mu\mathrm{m}$ for the edges of the tetrahedrons. The effective resolution of the mesh is comprised between the mean

tetrahedron height around 80 μmand the mean edge length of 100 μm. From the authors' experience, tetrahedron-based numerical methods have the same precision as hexahedron-based methods for the same resolution and the same order of truncation error. The main drawback of tetrahedrons comes from the fact that tetrahedron-based meshes count about eight times more elements than hexahedron-based meshes with the same resolution. The DNS mesh resolution is smaller than the laminar flame thickness based on the maximum temperature gradient $\delta_L = 424$ μm, thus ensuring to have ten points in a progress variable of the flame brush (Galpin *et al.*, 2008), and to resolve most of the turbulent scales away from the walls, since the estimated Kolmogorov length scale in the fresh gases is $\eta = 29$ μm. On the walls of the swirler, the first node in the fluid is approximately at $y^+ = 10$ and is thus in the viscous layer. The boundary layers are not resolved but they have a very limited impact on the flow.

The DNS computation required 16384 cores of an IBM Blue Gene/P machine during 80 hours to achieve a physical time of 1.9ms. This physical time is equivalent to the precessing vortex core characteristic time scale and to the turbulent eddy turnover time. Since this DNS computation was initialized with the converged solution of the finest LES of 329 million elements, the simulated physical time ensures that all the scales are converged in the DNS. The total CPU time for all the LES plus the DNS and all the post-processing is around 2.1 million CPU hours on the IBM Blue Gene/P system at IDRIS in France.

3.2 Flame structure

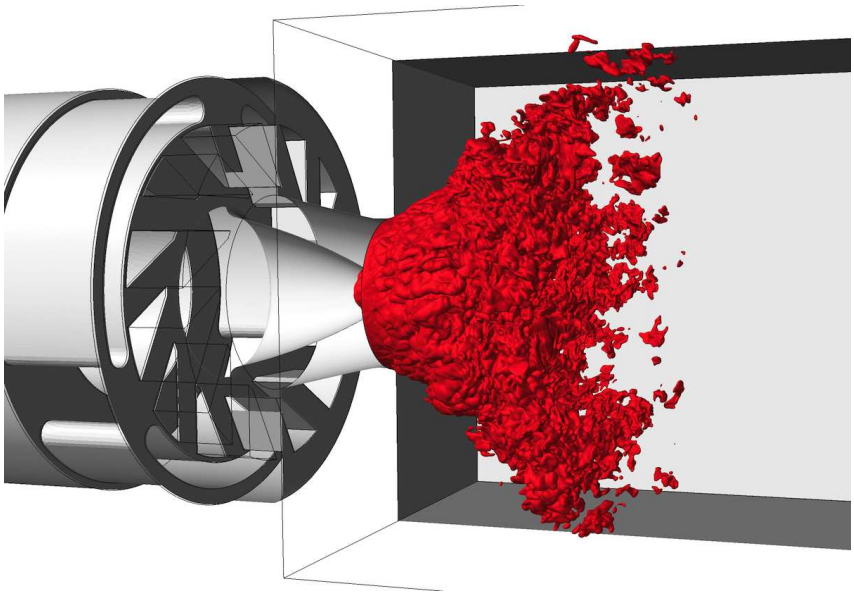

Figure 8: Iso-contour $c = 0.8$ of the progress variable in the DNS.

A 3D view of the $c = 0.8$ progress variable iso-surface is shown in Fig. 8. The flame has a V-shape with an anchoring on the head and the corners of the swirler. The wrinkling of the

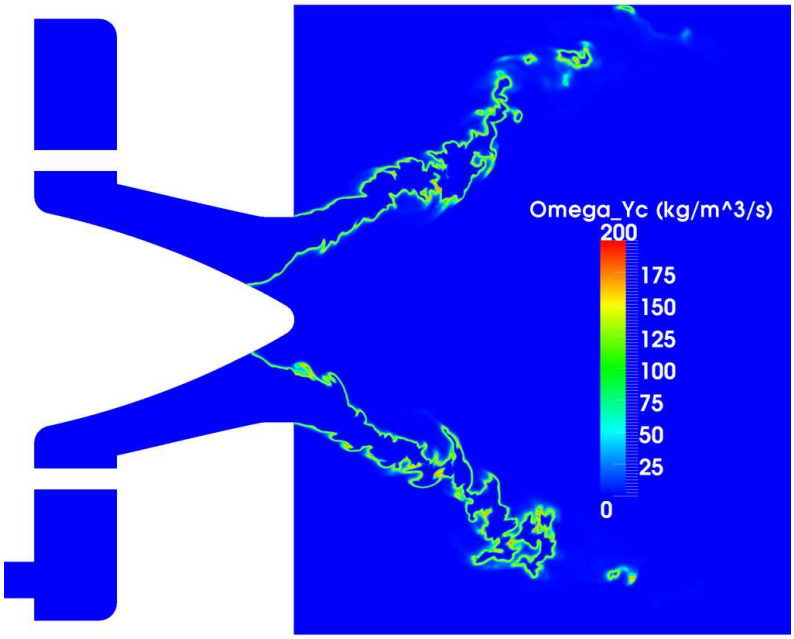

Figure 9: Progress variable source term in the median plane.

flame seems higher in the downstream locations with smaller structures. To give a better idea of the flame topology, the progress variable source term is plotted in the median plane in Fig. 9. As expected, the thickness of the source term varies between 300 $\mu\mathrm{m}$ and 1 mm, and is thus resolved on the mesh. The source term is thicker in the high wrinkling zones, that occur more likely in the downstream locations.

In the DNS, the OH radical may be post-processed from the chemistry table and compared to OH-LIF measurements performed at DLR. This comparison is presented in Fig. 10 with approximated color scales since the measurements are only qualitative. The filter resolution of the OH-LIF is around 350 $\mu\mathrm{m}$, while the DNS is around 100 $\mu\mathrm{m}$, thus explaining the smaller structures seen in the DNS. The opening of the flame is correctly reproduced in the DNS. The main difference comes from the OH-LIF intensity in the corner and central recirculation zones. This intensity is smaller in the corners and this is not observed in the DNS. This difference may be related to the temperature and CO concentration mismatch between measurements and LES computations exposed earlier.

Concerning the flame structure, the progress variable gradient gives a measure of the thickening of the flame due to turbulent scales entering the flame brush. This gradient and its standard deviation in the DNS are plotted against the gradient in the equivalent laminar flame in Fig. 11. For $c < 0.7$, the DNS gradient has smaller values than the laminar flame and an important standard deviation, indicating that the smallest vortices broaden the preheating region of the flame. For $c > 0.7$, which corresponds to the inner layer of the flame where most of heat release occurs, the gradients are similar, meaning that vortices are too large to penetrate into the inner layer.

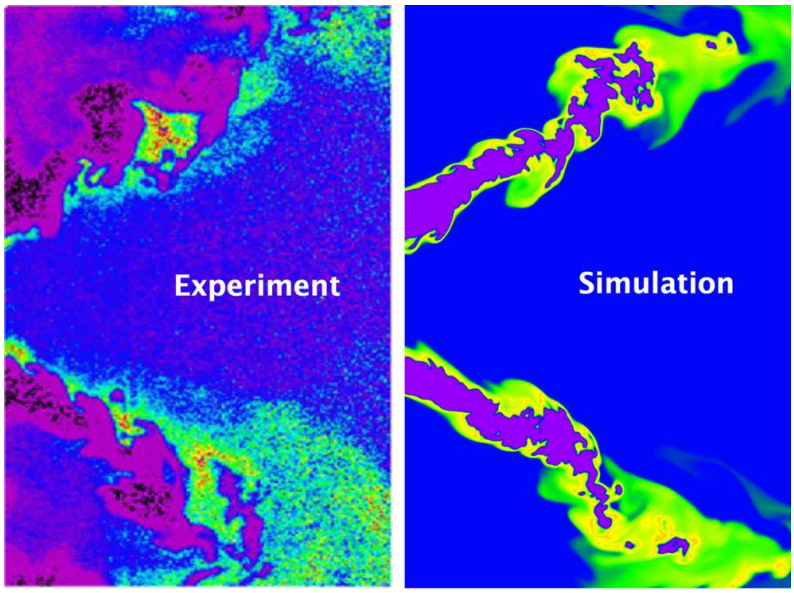

Figure 10: Comparison of OH-LIF measurement and OH concentration in the DNS.

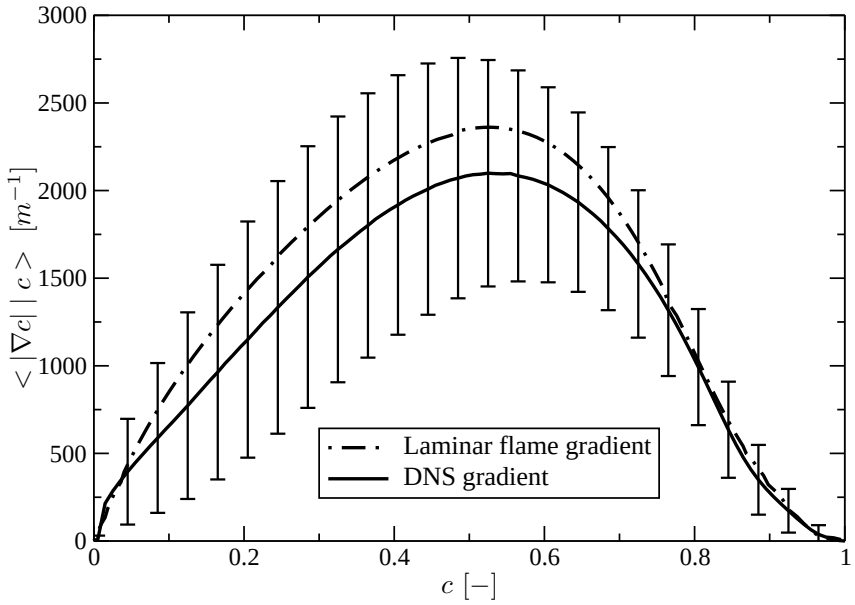

Figure 11: Progress variable gradient of the DNS compared to the laminar flame gradient. The error bars represent the standard deviation in the DNS.

This flame may thus be categorized in the thin reaction zones regime as stated in (Moureau *et al.*, 2007*b*). Moreover, the gradient standard deviation shows that the DNS gradient keeps values for which the stretch is limited. Stretched laminar flames, featuring the gradient of c

obtained in the DNS, were computed separately to be sure that these values of stretch do not affect the tabulated source term response of the progress variable CO + CO_2; even-though the observed stretch levels can have an impact on minor and intermediate species.

3.3 Filtering of the DNS fields

The DNS fields may be filtered at different filter width Δ to help in the design of LES models. The convolution with the filter kernel needed in the filtering process is trivial to implement for structured grids but it is far more complex for unstructured grids. Instead of discretizing the filter kernel on the unstructured mesh, another approach has been selected in this study. This method, which is based on a truncation of the moments of the filter, consists in expanding any variable to be filtered into Taylor series before performing the convolution. The convolution with the filter G on the domain $\mathcal{D}$ reads

$$\overline{\phi}(\mathbf{x}) = \int_{\mathcal{D}} G(\mathbf{y}-\mathbf{x})\phi(\mathbf{y})d\mathbf{y}\,. \tag{1}$$

In the 1D case, expanding $\phi(\mathbf{y})$ from the position $\mathbf{x}$ leads to the following expression

$$\overline{\phi}(\mathbf{x}) = \sum_{k=0}^{\infty} \frac{1}{k!}\mathcal{M}_k \frac{\partial^k \phi}{\partial x^k}(\mathbf{x})\,, \tag{2}$$

where $\mathcal{M}_k$ are the moments of the filter

$$\mathcal{M}_k = \int_{\mathcal{D}} \mathbf{y}^k G(\mathbf{y})d\mathbf{y}\,. \tag{3}$$

Instead of considering all the moments, the filtering may be achieved keeping only the first moments of the filter. Then, for a Gaussian filter in the 1D case, any variable ϕ filtered at Δ is simply written

$$\overline{\phi}(\mathbf{x}) = \phi(\mathbf{x}) + \frac{\Delta^2}{24}\frac{\partial^2\phi}{\partial x^2}(\mathbf{x}) + \frac{\Delta^4}{1152}\frac{\partial^4\phi}{\partial x^4}(\mathbf{x})\,. \tag{4}$$

This expression, which is similar to a diffusion equation, gives a simple mean to compute any filtered variable with differential operators available in finite-volume solvers. However, Eq. (4) must be computed as a series of sub-steps to alleviate the pseudo Fourier condition. This filtering technique has been validated on simple cases, where analytical solutions exist, as shown in Fig. 12. In this figure, a step function is filtered at different filter widths Δ, and the computed profiles are compared to the analytical solutions given by $(1+\mathrm{erf}(\sqrt{6}\,\mathrm{x}/\Delta))/2$ for a Gaussian filter. In the figure, the computed and analytical profiles are hardly distinguishable. Thus, the DNS fields were filtered with this technique, at 4, 8, 16, and 32 times Δ_{DNS}.

3.4 Multi-scale analysis

The first point that was analyzed with this filtering technique, is the sub-filter unmixedness factor for the Favre and Reynolds progress variables, that is presented in Fig. 13. This factor is

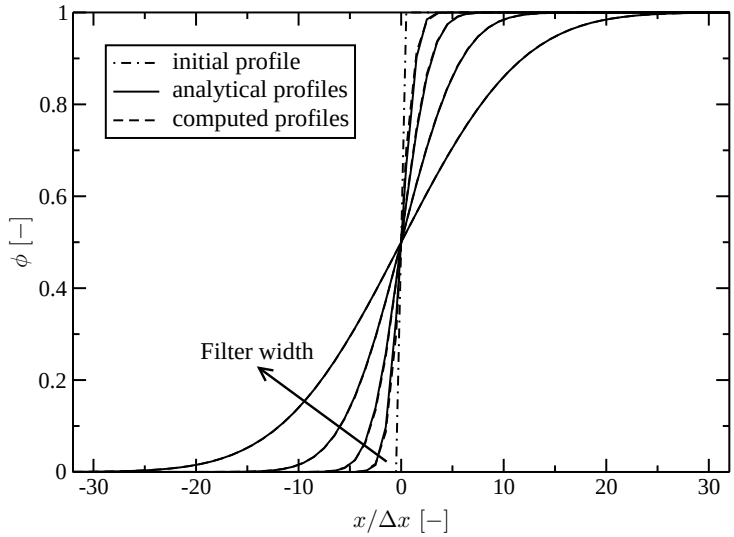

Figure 12: Filtering of a step function. The filter width Δ takes the values 4, 8, 16 and 32 times the mesh resolution Δx.

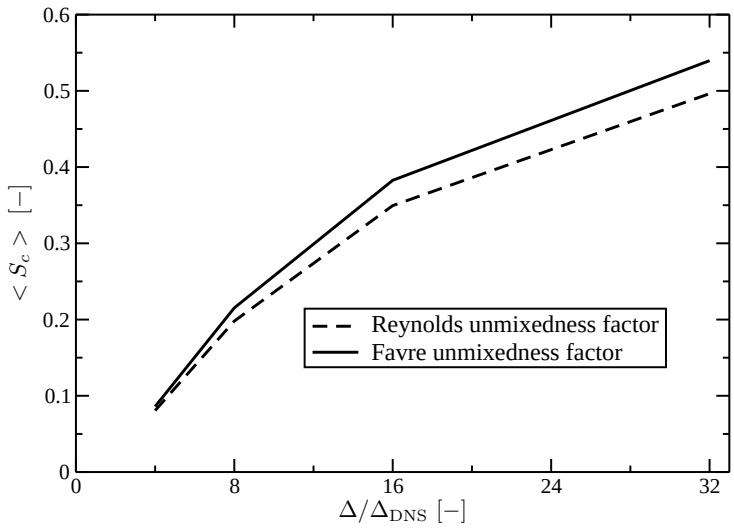

Figure 13: Unmixedness factor of the Favre and Reynolds progress variables from the filtered DNS as a function of the filter width.

expressed as the domain averaged of $S_{\tilde{c}} = (\widetilde{c^2} - \tilde{c}^2)/(\tilde{c}(1-\tilde{c}))$ conditioned by $0.1 < \tilde{c} < 0.9$ for the Favre filtering and $S_{\overline{c}} = \overline{c^2} - \overline{c}^2/(\overline{c}(1-\overline{c}))$ conditioned by $0.1 < \overline{c} < 0.9$ for the Reynolds filtering. These factors, that have similar trends, increase sharply for small filter widths and become close to unity for the large ones.

The second point that was addressed is the sub-filter wrinkling of the flame front. In Fig. 14, the sub-filter wrinkling $\overline{|\nabla c|}/|\nabla \overline{c}|$ conditioned by the Reynolds filtered progress variable $\overline{c}$ and

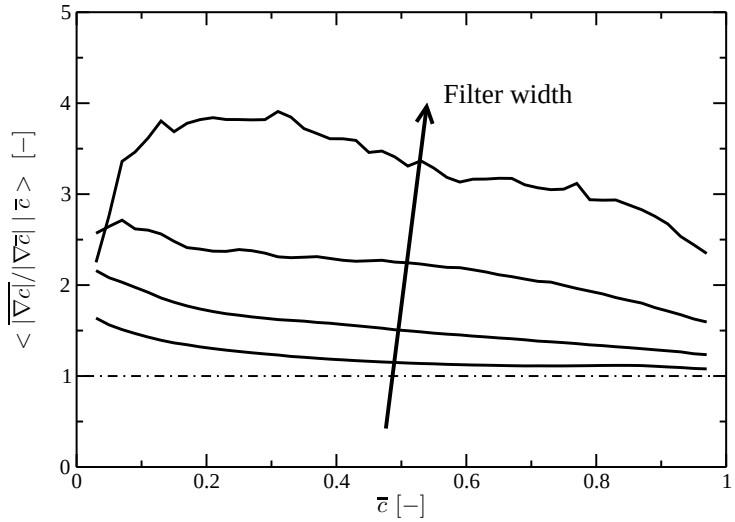

Figure 14: Subfilter wrinkling of the flame brush conditioned by $\overline{c}$. $\Delta = 4$ to $32\Delta_{\mathrm{DNS}}$.

averaged on the whole domain is plotted. As expected, the sub-filter wrinkling is close to unity for the smallest filter widths and increases with the filter width. This wrinkling may reach important values and is not necessarily constant as a function of $\overline{c}$ for the largest filter width.

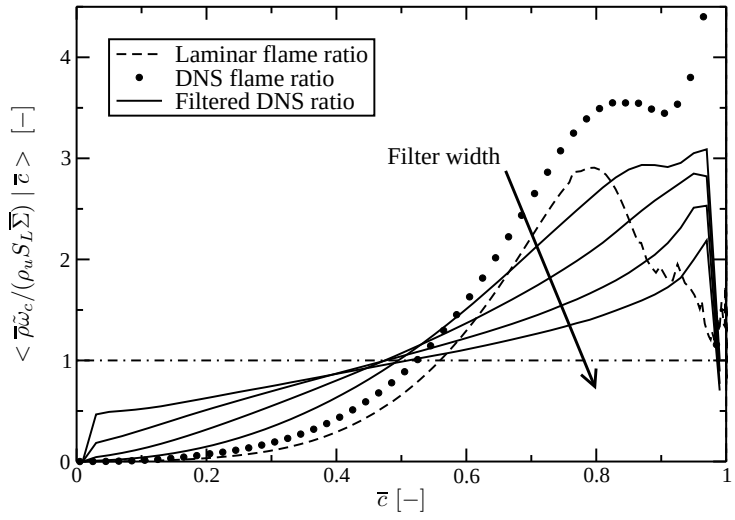

Figure 15: Ratio of the filtered source term and the flame surface density. $\Delta = 4$ to $32\Delta_{\mathrm{DNS}}$.

Another important quantity for the understanding of the flame structure at different levels is the ratio of the filtered source term $\overline{\rho}\widetilde{\omega}_c$ and the flame surface density multiplied by the intrinsic momentum of the flame $\rho_u S_L \overline{\Sigma} = \rho_u S_L \overline{|\nabla c|}$. This term appears when filtering and normalizing the balance equation for the progress variable, that may be cast in $\rho(\partial_t c + u \cdot \nabla c) =$

$\nabla \cdot (\rho D \nabla c) + \rho \dot{\omega}_c = \rho V_c |\nabla c|$, with usual notations, and where V_c is the relative progression velocity of the iso-c surface. In an unstrained one-dimensional laminar flamelet, $\rho V_c = \rho_u S_L$. Coherent flame models for RANS, for instance, suppose that the averaged molecular diffusion term is negligible and that the source term ratio should be unity. In Fig. 15, this ratio is plotted for different filter widths and compared to the DNS ratio and to the laminar flame ratio. The DNS and laminar flame ratios as well as the ratios for small filter widths are far from unity because, in these cases, the source term is the balance between the transport term $\rho_u S_L \overline{\Sigma}$ and other terms of the above c-equation that come from diffusion of the progress variable or from the local stretch responsible for a departure between ρV_c and $\rho_u S_L$. When the filter width increases, the transport term becomes dominant and the ratio finally tends towards unity recovering the RANS current hypothesis.

3.5 A priori evaluation of the PCM-FPI model

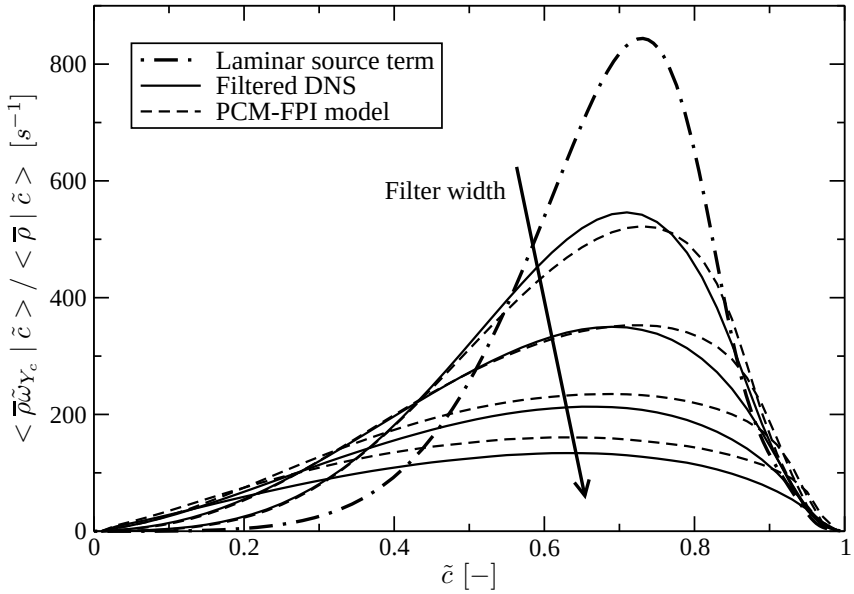

Figure 16: Comparison of the conditioned progress variable source term from the DNS and from the PCM-FPI chemistry table. The source term is conditioned only by the filtered progress variable. $\Delta = 4$ to $32\Delta_{\mathrm{DNS}}$.

The filtering of the DNS fields allows to extract many valuable informations for the validation of existing combustion models, or to propose new ones. As a first step, the PCM-FPI (Domingo *et al.*, 2008; Gicquel *et al.*, 2000; Van Oijen *et al.*, 2001), which is used in the LES computations of this study, is validated a priori with this DNS. The validation is performed by comparing the filtered source term of the progress variable $\widetilde{\omega}_{Y_c}$ to the one given by the PCM-FPI chemistry table, which is a function of the local filtered progress variable $\tilde{c}$ and the unmixedness factor $S_{\tilde{c}}$. The comparison is presented in Fig. 16. In this figure, the DNS and PCM-FPI source

terms are conditioned on $\tilde{c}$ before accumulating Favre averages. The agreement between the filtered DNS and the model is satisfactory, and the presumed beta-pdf correctly reproduces the flattening of the source term in the case of large unmixedness factors with some over-estimation, that may lead to a slight over-prediction of the flame speed. In this test, the SGS variance is exactly computed from the DNS field, therefore the departure observed is the smallest that could be found in LES, where the SGS variance may be subjected to additional errors, for instance introduced by scalar dissipation rate modeling if a balance equation is solved (Domingo *et al.*, 2008).

4 Conclusion

In this paper, LES and DNS of an industrial swirl burner are presented and analyzed. This type of database, which is among the largest ones from the authors' knowledge, associated with appropriate post-processing tools is extremely useful for the validation of existing models, like the PCM-FPI model, or the design of new combustion models. Still, this DNS has some limitations, especially concerning the treatment of heat transfers in the corner recirculation zones, or the partial premixing that is observed in the experiments. All these phenomena should be added to have a totally representative database.

Acknowledgments

Dr. Meier and his team from DLR are gratefully acknowledged for providing the details of the experimental results. The authors acknowledge the support of the French National Research Agency (ANR) through the funding of the SIMTUR project. This work was granted access to the HPC resources of IDRIS under the allocation 2009-020152 made by GENCI (Grand Equipement National de Calcul Intensif). The authors also thank Guillaume Lodier for the stretched flames computations.

References

Domingo, P., Vervisch, L. & Veynante, D. (2008), Large-eddy simulation of a lifted methane jet flame in a vitiated coflow. *Combustion and Flame* **152** (3), 415 – 432.

Galpin, J., Naudin, A., Vervisch, L., Angelberger, C., Colin, O. & Domingo, P. (2008), Large-eddy simulation of a fuel-lean premixed turbulent swirl-burner. *Combustion and Flame* **155** (1-2), 247 – 266.

Germano, M., Piomelli, U., Moin, P. & Cabot, W. H. (1991), A dynamic subgrid-scale eddy viscosity model. *Phys. Fluids* **3** (7), 1760–1765.

Gicquel, O., Darabiha, N. & Thévenin, D. (2000), Laminar premixed hydrogen/air counterflow flame simulations using flame prolongation of ildm with differential diffusion. *Symposium (International) on Combustion* **28** (2), 1901 – 1908.

Lartigue, G., Meier, U. & Bérat, C. (2004), Experimental and numerical investigation of self-excited combustion oscillations in a scaled gas turbine combustor. *Applied Thermal Engineering* **24** (11-12), 1583 – 1592.

Meier, W., Weigand, P., Duan, X. & Giezendanner-Thoben, R. (2007), Detailed characterization of the dynamics of thermoacoustic pulsations in a lean premixed swirl flame. *Combustion and Flame* **150** (1-2), 2 – 26.

Moureau, V., Bérat, C. & Pitsch, H. (2007*a*), An efficient semi-implicit compressible solver for large-eddy simulations. *Journal of Computational Physics* **226** (2), 1256 – 1270.

Moureau, V., Minot, P., Pitsch, H. & Bérat, C. (2007*b*), A ghost-fluid method for large-eddy simulations of premixed combustion in complex geometries. *Journal of Computational Physics* **221** (2), 600 – 614.

Poinsot, T. & Veynante, D. (2001), *Theoretical and Numerical Combustion*. Philadelphia: R. T. Edwards, Inc.

Rivara, M.-C. (1984), Mesh refinement processes based on the generalized bisection of simplices. *SIAM Journal on Numerical Analysis* **21** (3), 604–613.

Roux, S., Lartigue, G., Poinsot, T., Meier, U. & Berat, C. (2005), Studies of mean and unsteady flow in a swirled combustor using experiments, acoustic analysis, and large eddy simulations. *Comb. Flame* **141** (1-2), 40–54.

Smith, G. P., Golden, D. M., Frenklach, M., Moriarty, N. W., Eiteneer, B., Goldenberg, M., Bowman, C. T., Hanson, R. K., Song, S., Gardiner, W. C., Lissianski, V. V. & Qin, Z. (1999), *Tech. Rep.*. http://www.me.berkeley.edu/gri-mech/.

Van Oijen, J. A., Lammers, F. A. & de Goey, L. P. H. (2001), Modeling of complex premixed burner systems by using flamelet-generated manifolds. *Combustion and Flame* **127** (3), 2124 – 2134.